University of Thi-Qar Journal of Science (UTJsci)
E-ISSN: 2709-0256, P-ISSN: 1991-8690, Vol. 11, No. 1, Jun. 2024

Investigation of Saturable Absorber Length Effect on Characteristics of Passive Q-Switching and Stokes with Anti-Stokes Pulses Generated in Laser System of Nd:YVO4

Dunya Saad Hussein*[1a], Abdul-Kareem Mahdi Salih [1b] , Rasool Asal [2c]

[1] *Dept. of Physics, College of* Science, *University of Thi-Qar, Thi-Qar, Iraq.*
2Sesar Lab,University of Milan,Italy

[b]E-mail: karimmahdisalih@yahoo.co.uk
[a*]Corresponding author: matrix199408@gmail.com
[c]rraa5085@gmail.com

Received: 2023-12-10, Revised: 2024-01-19, Accepted: 2024-01-24, Published: 2024-06-01

***Abstract*— The effect of the saturable absorbent material on the characteristics of Passive Q-Switching and Stokes with Anti-Stokes Pulses Generated in Laser System of Nd:YVO4 has been investigated.**. The three **pulses (passive Q-switching pulse, Stokes pulse, and anti-Stokes pulse) simultaneously generated from one optical system. The optical system consists of Nd: YVO4, PbWO4, and Cr + 4: YAG as an effective medium, Raman medium and saturable absorbent material, respectively. The modeling of the rate equations was used, and the Rung-Kutta-Fehelberg numerical method was used to solve the rate equations. The results show increased power of the pulses generated, requiring an increased length of the saturable absorber material used in the system. The results showed that at the shortest length used for the saturated absorbent material, the pulse duration and energy of the three generated pulses were PQS pulse (16.44ns, 1.39mJ), Stokes pulse (12.59ns, 1.148mJ) and anti-Stokes pulse (13.53ns, 1.59mJ), while at the longest length of the saturated absorbent material, the pulse duration and energy were PQS pulse (14.68ns, 1.50mJ), the Stokes pulse (11.41ns, 1.36mJ) and the anti-Stokes pulse (12.38ns, 1.86mJ).**

***Keywords*— Cr^{+4}: YAG, Laser, passive Q-switching pulse, Raman medium**

I. INTRODUCTION

The technology chosen to produce brief pulses with high peak power is Q-switching. Since large laser pulses may be produced using the passive Q-switching method [1]. By allowing the pumping process to build up a population inversion and gain inside the laser cavity without oscillations, which are larger than the typical values under free-running operation, It can be illustrated through fig.1 [2,3].

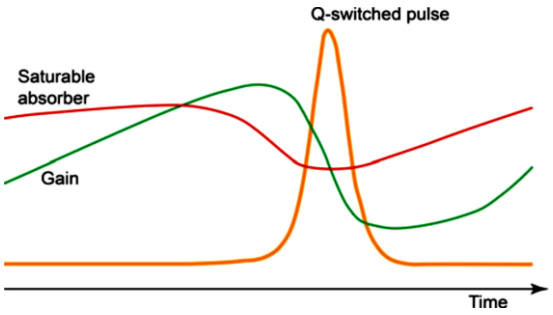

Figure 1: Dynamics of a passively Q-switched laser[3]

The low cost and straightforward design of passive Q-switching (PQS) make it a popular technique for producing nanosecond pulses[4] , while the mode-locking technique produces picosecond pulses. In the PQS technique, the laser photon oscillation is prevented until the population inversions reach a value greater than the total optical losses inside the cavity. This is achieved by placing saturable absorber material (SA) with strong absorption at the laser wavelength inside the laser resonator. In the initial time, the SA is characterized by high activity of photons absorption because of the high ions population in the ground state, with reaching saturation case, when the population of the excited state becomes greater than the population of the ground state. PQS solid-level lasers are vital for many uses, including nonlinear optical investigations, medical equipment, pollution sensors, range finders, lidars, and laser drilling and cutting [5]. The most widely used SA is $Cr^{4+:\,YAG}$ crystal due to the good optical and thermal properties of YAG [6]. As seen in Figure (2A) [7], the Cr^{+4} ion also has a low saturation effect of around 1064 nm and a reasonably high absorption cross-section. As seen in Figure (2B), the SA of Cr^{+4}: YAG is a conventional four-level system [8]. The system has two absorption paths from the ground levels (E_1

https://doi.org/10.32792/utq/utjsci/v11i1.1146

)to E_3 and from the excited levels (E_2) to E_4, these absorptions are represented by the ground level absorption cross section σ_{gs} and excited level absorption cross section σ_{es}. The lifetime (τ_s) is determined by the relaxation from the excited level to the ground level, τ_s of the levels E_3 and E_4 are assumed to be very short, therefore the excited level absorption represents the non saturable loss. The fast transition of ions from E_3 to E_2 level leads to the increase the ions accumulation in E_2 more than E_1 and thus the SA arrives to the bleaching state. Thus, it allows the laser pulses to be released at earlier time. The parameters, σ_{gs}, σ_{es}, and τ_s, can well describe the dynamics of the SA [8]. An important third-order nonlinear phenomenon is stimulated Raman scattering (SRS) [9]. A few theoretical investigations to the effect of anti-Stokes pulse with ultra-short pulse passive Q-switching [10]. Furthermore, some research uses the Stokes pulse for passive Q-switching [11]. Because of their intriguing physical characteristics and wide range of uses, the structural level compounds $CaWO_4$, $SrWO_4$, $BaWO_4$, and $PbWO_4$ have been the subject of intense research over the past years [12]. Suitable active materials for Raman lasers include $PbMoO_4$ and $PbWO_4$, which are crystals that self-activate when exposed to ions from rare earth lasers [13]. $PbWO_4$ is one of these crystals that have excellent potential for use in Raman lasers due to its inexpensive cost, ease of growth, broad transmittance spectrum, high optical damage threshold, and big gain coefficient. The $PbWO_4$ Raman has been the subject of substantial investigation [14].

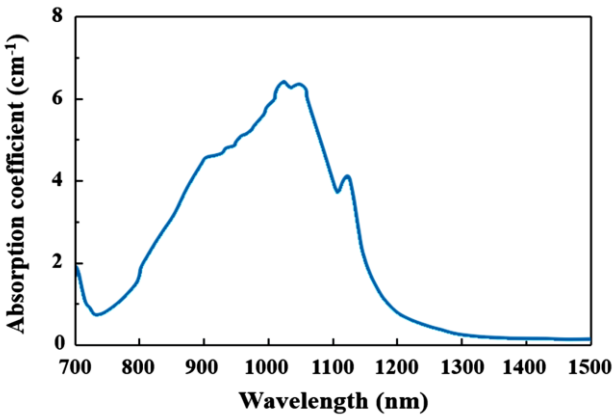

Figure 2A : Absorption spectrum of Cr^{4+}:YAG[7]

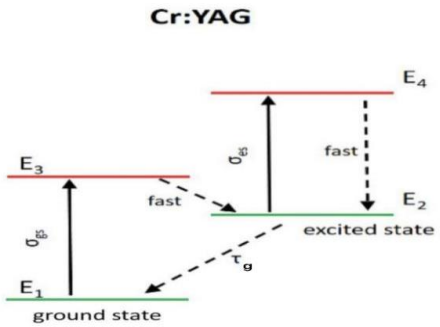

Figure 2B :Energy level of Cr^{+4}:YAG[8]

II. THEORY

First, confirm that you have the correct template for your paper size. This template has been tailored for output on the A4 paper size. If you are using US letter-sized paper, please close this file and download the Microsoft Word, Letter file.

A mathematical rate equations model [15], as shown in Equations (1-6) has been used to study the effective of the SA length on characteristic of PQS, Stokes and anti-Stokes pulses where generated simultaneously in optical laser system.

$$\frac{d\emptyset_L}{dt} = \emptyset_L\left[k_g N_g - k_a N_{ag} - \beta k_a N_{ae} - \frac{2ghcv_s\emptyset_s l_R}{\tau_{Rt}} - \frac{2ghcv_{as}\emptyset_{as} l_R}{\tau_{Rt}} - \frac{1}{\tau_L}\right] \quad (1)$$

$$\frac{d\emptyset_S}{dt} = \emptyset_S\left[\frac{2ghcv_s\emptyset_L l_R}{\tau_{Rt}} - k_a N_{ag} - \beta k_a N_{ae} - \frac{1}{\tau_S}\right] + K_{SP}\emptyset_L \quad (2)$$

$$\frac{d\emptyset_{as}}{dt} = \emptyset_{as}\left[\frac{2ghcv_{as}\emptyset_L l_R}{\tau_{Rt}} - k_a N_{ag} - \beta k_a N_{ae} - \frac{1}{\tau_{as}}\right] + K_{SP}\emptyset_L \quad (3)$$

$$\frac{dN_g}{dt} = R_p - \gamma_g N_g - \gamma_p k_g N_g \emptyset_L \quad (4)$$

$$\frac{dN_{ag}}{dt} = -K_a N_{ag}\emptyset_L - k_a N_{ag}\emptyset_s - k_a N_{ag}\emptyset_{as} + \gamma_a N_{ae} \quad (5)$$

$$\frac{dN_{ae}}{dt} = K_a N_{ag}\emptyset_L + K_a N_{ag}\emptyset_s + k_a N_{ag}\emptyset_{as} - \gamma_a N_{ae} - \beta K_a N_{ae}(\emptyset_s + \emptyset_{as}) \quad (6)$$

Equations 1, 2 and 3 describe the time variation of laser photons density, Stokes photons density and anti-Stokes photons density respectively. The Equation 4 describes the population inversion density and Equations 5 and 6 describe the time variation of population of the SA ground and excited level receptivity. $\emptyset_L$ (cm^{-3}) Laser photons density. $K_g = \frac{2l_g\sigma_g}{\tau_{Rt}}(s^{-1})$ coupling coefficient $L_g(cm)$,is length of active medium, $\sigma_g(cm^2)$ is the emission cross section of active medium , N_g (cm^{-3}) is the population inversion density, $\tau_{Rt} = \frac{2l_c}{c}$ (s) is the life time of photon in cavity $K_a = \frac{2L_a\sigma_{ag}}{\tau_{Rt}}$ (s^{-1}) , is coupling coefficient between the photons and saturable absorber material, l_c (cm) is cavity length, σ_{ag} (cm^2) the absorption cross section of ground level of SA, L_a is length of SA ,N_{ag} is population of ground level in SA (cm^{-3}), $\beta = \frac{\sigma_{ae}}{\sigma_{ag}}$, $\sigma_{ae}(cm^2)$ is the absorption cross of excited level of SA, N_{ae} (cm^{-3}) is the population of excite level in SA, $N_{ag} + N_{ae} = n_i$, where n_i is the total ions density (concentration) of SA, g is the Raman gain (*cm*/GW) , h plank constant ,c $(cm/s)$is the speed of light in vacuum , $v_s(cm^{-1})$ the frequency of Stokes photon , $v_s = v_L - v_R$, v_L laser frequency v_R is the Raman

shift , l_R is Raman medium length, v_{as} is the anti-Stoke photon frequency, $v_{as} = v_l + v_R$, $\tau_L$is the life time of laser photon in the cavity $\tau_L = \frac{2L_C}{c[L-ln\sqrt{RR_L}]} = \frac{\tau_{RT}}{[L-\ln(\sqrt{RR_L})]}$, $L(cm)$ is the round trip losses in the cavity, $\emptyset_S$ *is* Raman-Stokes photons density, k_{sp} is the spontaneous Raman scattering factor (s^{-1}), R_p (s^{-1}) is the pumping rate, $\gamma_g = \frac{1}{\tau_g}$ (s^{-1}) is the decay rate of the upper laser level (excited level), τ_g (s) is the life time of excited level, $\gamma_p$is population reduction $\gamma_p = 2$ for 3 level system, $\gamma_p = 1$ for 4 level system, R is the reflectivity of total reflection mirror, $R_L$is the output coupler reflectivity at laser photon , $\tau_s = \frac{2L_C}{c[L-ln\sqrt{RR_s}]}$ is the round trip losses of Stokes photons of the cavity, R_s is output coupler reflectivity at stokes photons, $\tau_{as} = \frac{2L_C}{c[L-ln\sqrt{RR_{as}}]}$ is the round trip losses of anti-Stokes photons in the cavity , R_{as} is output coupler reflectivity at anti-Stokes. It is worth noting, it is imperative to make some physical and mathematical approximation. The first and the second term in Equation 4 can be neglected due the release and emission of PQS pulse in very short time compared to the time influence of the factors R_p , γ_g[16, 17], also the fourth term in the Equation 5, and the fourth and the fifth terms in Equation-6 can be neglected due to long time decay of excited level of the SA, level 2 and due to very short lifetime of level 4 [18]. At initial time of construction of PQS pulse, the Equation 1 can be approaching to zero ($\frac{d\phi_L}{dt} \approx 0.$), $N_{ae} \approx 0.$, $N_g = N_{go}$, $N_{ag} \approx n_i$, then it is possible to appreciate the initial population inversion density N_{go} as the following expression:

$$N_{g0} = \frac{k_a N_{ao} + (^{(2ghc\, l_R(v_s\emptyset_s + v_{as}\emptyset_{as})}/_{\tau_{RT}}) + \frac{1}{\tau_L}}{K_g} \qquad (7)$$

Also at the time that PQS pulse at its peak, Equation 1 can be approaching to zero ($\frac{d\phi_L}{dt} \approx 0.$), $N_{ag} \approx 0.$, $N_g = N_{th}$, $N_{ae} \approx n_i$, then it is possible to estimate the threshold population inversion density N_{th} as the following expression:

$$N_{th} = \frac{\beta K_a N_{a0} + (^{(2ghc\, l_R(v_s\emptyset_s + v_{as}\emptyset_{as})}/_{\tau_{RT}}) + \frac{1}{\tau_L}}{k_g} \qquad (8)$$

After the pulse is released, it can estimate the pulse energy (E) as the following expression [19]:

$$E = \frac{(N_{go} - N_{gf})}{N_{go}} \frac{(N_{go} - N_{gf})h\nu}{\gamma} \qquad (9)$$

Where N_{gf} represents the final value of population inversion density, it can be determined from the results of the numerical solution of Equation 4, and h Blank constant, v is the frequency. The duration of pulse (τ) as well as can be estimated after the pulse released (from numerical solution results of Equation 1, 2, 3), it is represents the pulse width at half maximum (FWHM). The power calculates by the relation:

$$P = \frac{E}{\tau} \qquad (10)$$

III. Results and Discussion

The set of rate equations (1-6) solves numerically by Rung-Kutta-Fehelberg method, table 1 shows the input data that has been used in computation:

Table 1: Input data of computations

Parameter	Value	Ref.
K_{sp}	$2 \times 10^{-10} s^{-1}$	
v_R	$925\ cm^{-1}$	
G	8.4*cm*/GW	[20]
σ_e	$6.5 \times 10^{-19} cm^2$	[21]
σ_{ae}	$0.55 \times 10^{-18} cm^2$	[22]
σ_{ag}	$2.5 \times 10^{-18}\ cm^2$	

Figure 3 shows an increase in the initial population inversion density (IPID) of ions with the increase of length of SA material (L_a).

The study explains that related to a decrease in the laser photons density inside the optical cavity due to the increase in the absorption activity of saturable absorber material, that lead to less ions-photons interaction to be caused ions accumulation in upper laser state**.** Figure 4 shows the increments of threshold population inversion density (TPID) while the increment of saturable absorber population density.

The study gives reason to increment which occurred in IPID which is discussed in Figure 3. The Figure 5 shows the increase the difference between the initial and final value of population inversion density (difference population inversion density (DPID). It is worth noting that in despite of the increasing in final value of population inversion density (FPID) as shown in Figure 6.

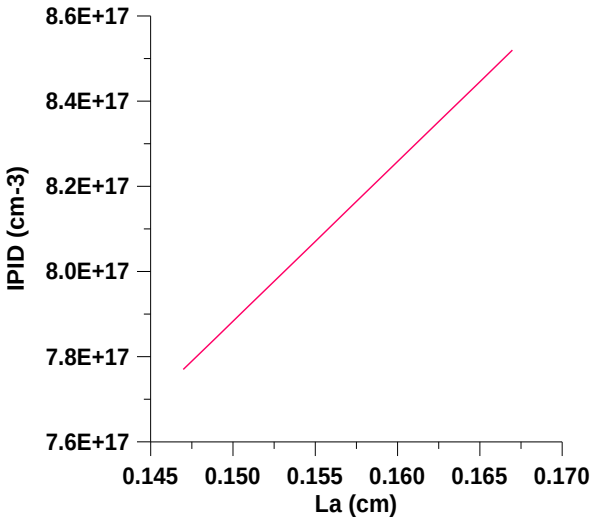

Figure 3: IPID as a function of L_a

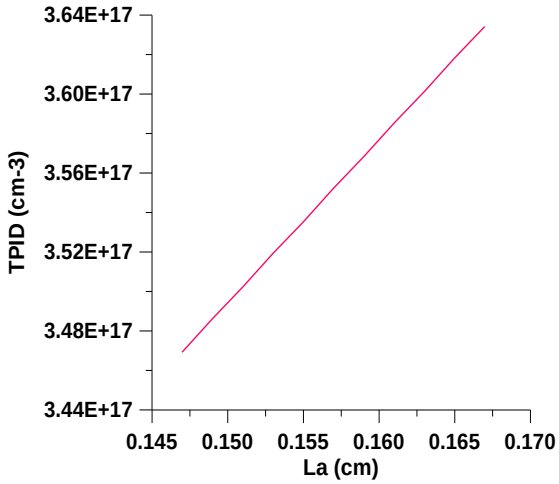

Figure4: TPID as a function of L_a

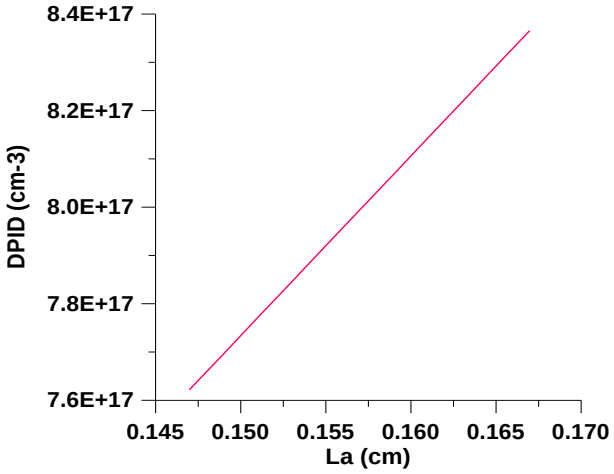

Figure 5 : DPID as a function of L_a

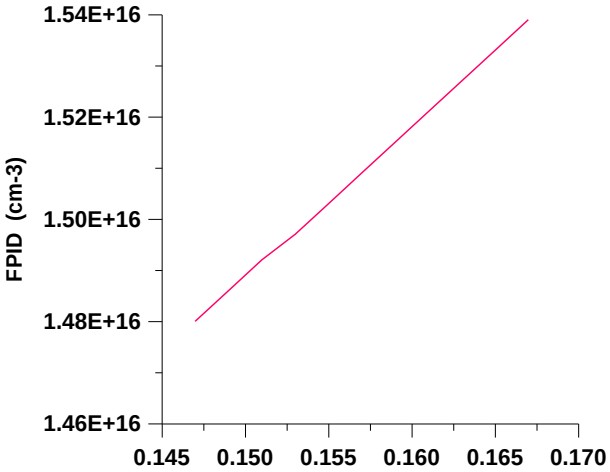

Figure 6 : FPID as a function of L_a

The difference between the initial and final values still increases. The increase in the final value is less than the increase in the initial value, which makes the increment in difference lead to an increase in the maximum photon density (MPD), as shown in Figure7.

Figure8 shows that the increase in L_a causes an increase in the energy of the essential pulse (passive Q-switching pulse) Stokes pulse and anti-Stokes pulse, the reason is the increasing values of the IPID indicated in Figure 3 yield an increase in MPD in Figure 7.

The occurrence of increase in energy accompanied with decay in duration for generated pulses as shown in Figure 9 make available to get pulses with high power as shown in Figure10.

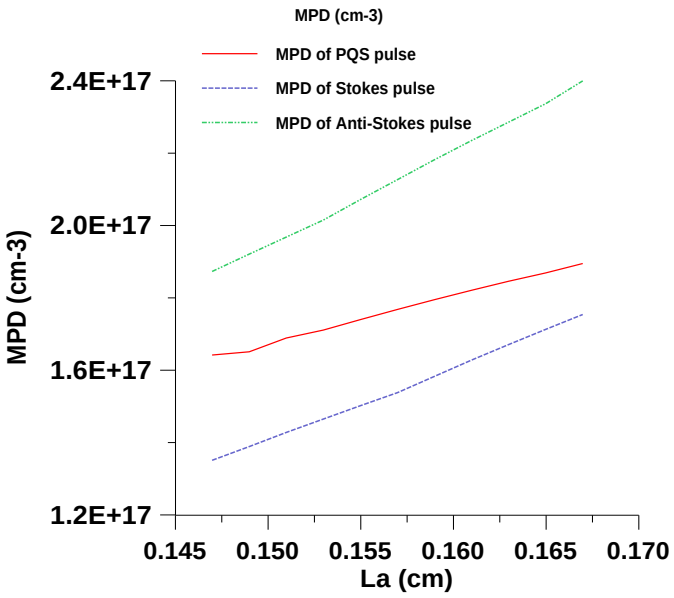

Figure 7: MPD of pulse as a function of L_a

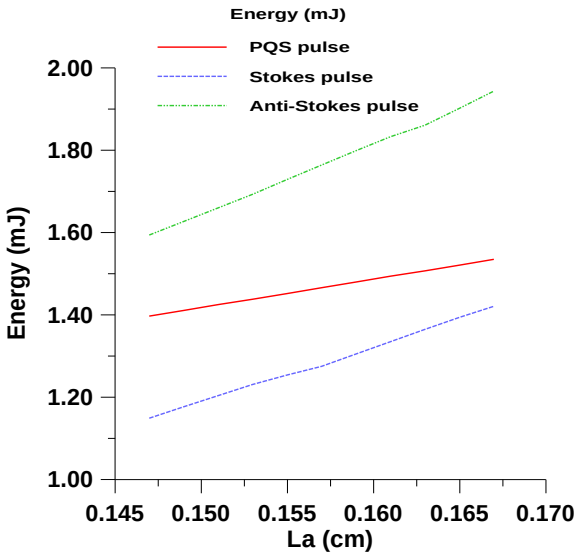

Figure 8 : Energy of pulse as a function of L_a

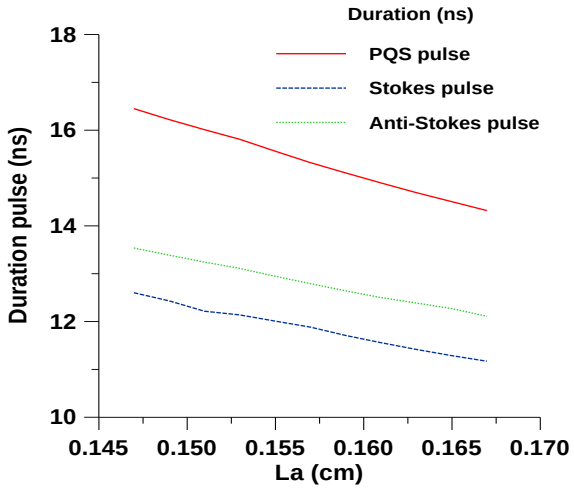

Figure 9 : Duration pulse as a function of L_a

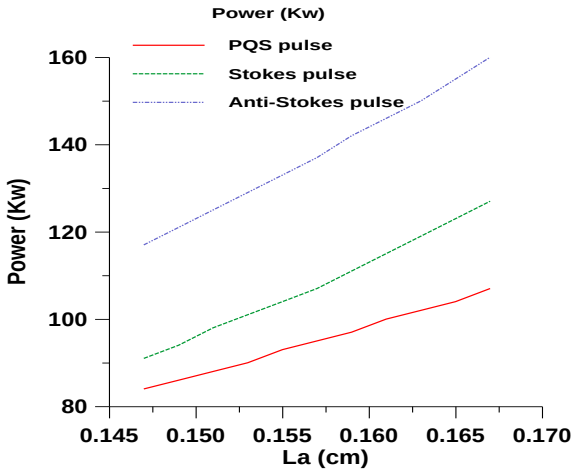

Figure 10 : Power pulse as a function of L_a

Figures 11 and 12 show the pulse behavior of three pulses generated in the difference, where the PQS photons density in Figure 11 appears increasing with increasing L_a as shown in table 2, the peak of Stokes photons density is decreasing, while the peak of anti- Stokes photons density increases to maximum value comparison with other pulse. Figure 12 shows increase the peak of photons density of PQS pulse with increase L_a and decrease the peak of photons density of Stokes photon density while increasing of photons density of anti-Stokes pulse. From the results of the study, it can be noticed that the anti-Stokes pulse began to increase compared to the other pulses, because a large number of Raman medium ions is located on the upper (final) energy state of Raman medium, the transition of this ions to lower (initial) energy state causes the emission of pulse with high intensity. In comparing between Figure 11 and Figure 12, it can be noticed that the peak of pulses occurs at advance time when the La increases as shown in table 2.

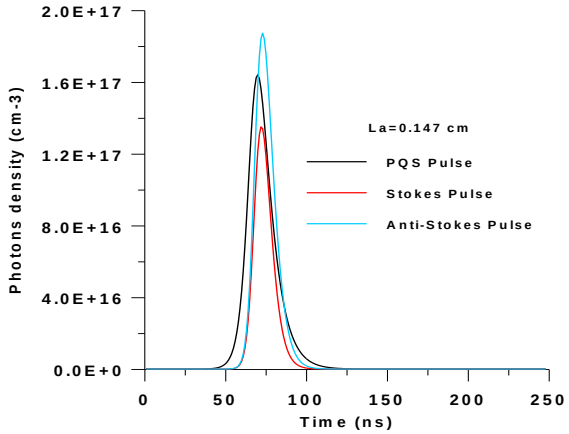

Figure 11:The profile PQS , Stokes , anti- Stokes at L_a= 0.147 cm

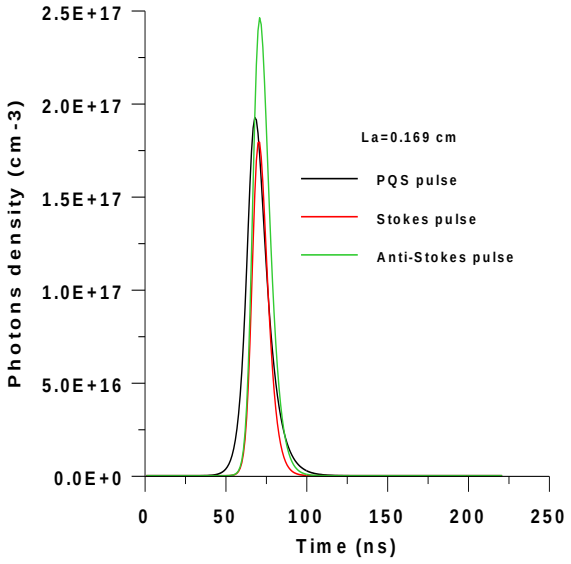

Figure 12: The profile PQS , Stokes , anti- Stokes at L_a=0.147 cm

Table 2: Maximum photons density for pulses with the time

Maximum photons values of pulses at L_a=0.147cm				Maximum photons values of pulses at L_a=0.169 cm		
Pulse type	PSQ	Stokes	Anti-Stokes	PSQ	Stokes	Anti-Stokes
Photons density (cm^{-3})	2.2×10^{17}	1.4×10^{17}	2.8×10^{17}	2.8×10^{17}	2.6×10^{17}	2.9×10^{17}
Time(ns)	75	77	79	70	75	78

Figure13 and 14 are show the profile of photons density and PID of two values of L_a. The behavior show increase the photons density and PID with increase L_a, at the initial time slowly and gradual growth in photon density of pulse due to high efficiency of SA activity. The increase of $L_{a\ gives}$ a good chance for active medium ions which exist in a low energy state for absorbing the optical pumping photons and transferring into high energy states. This transfer lead to fulfill population inversion state till reaching the maximum value before the SA activity decreases to reach the optical bleaching state.

.

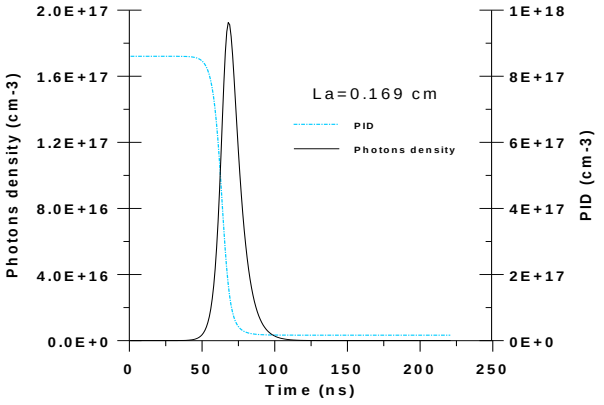

Figure 13: The profile of photons density and PID at L_a=0.169 cm

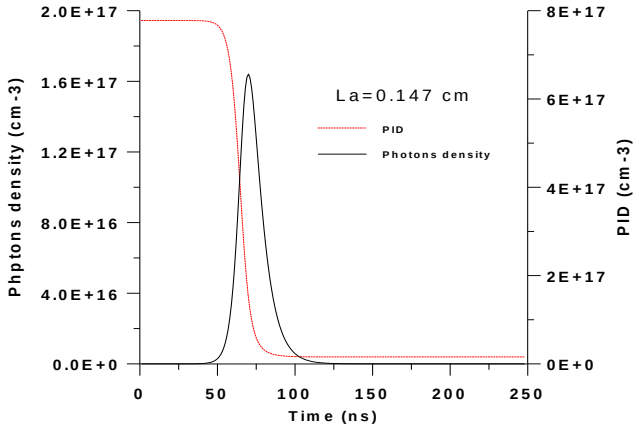

Figure 14: The profile of photons density and ,PID at L_a= 0.147 cm

IV. Conclusion

The study shows how to control the power of pulses by controlling the length of saturable absorber material. The study reached the following conclusions: increasing L_a leads to an increase in IPID, DPID, and MPD. On the other hand, it leads to a decrease in pulse duration for PQS, Stokes and anti- Stokes pulse. Thus to increase the power of the generated pulses it must increase the length of SA that is used in system. With the comparison with ref. [23], the duration pulse of PQS in microseconds is about (8.55–3.43) μs, while in our study in nanoseconds (16.44 ns); it was given a very short pulse. The pulse that is shorter than the pulse of the mentioned source, it generates high power for pulses.

Conflict of interest

Authors declare that they have no conflict of interest.

REFERENCES

[1] L.Lu, J. CHENG, Q. ZHAO,J ZHANG, H. YANG, Y. ZHANG, Z. HUI, F. ZHAO and W. LIU3, "Chromium oxide film for Q-switched and mode-locked pulse generation." *Optics Express*, Vol. 31, No. 10, p.p16872-16881, 2023.

[2]C. Perrière , R. Boulesteix ' A. Maître , B. Forester, A.iJa locha , A. Brenier. "Study of dopant distribution in Cr^{+4}: YAG transparent ceramics and its use as passively Q-switching media in Nd: YAG laser delivering 38 mJ per pulse." *Optical Materials: No.*12 ,p.p 100107, 2021 .

[3] K.. Ursula, and R. Paschotta. "Ultrafast Lasers."*Springer International Publishing*,. https://doi.org/10.1007/978-3-030-82532-4, 2021.

[4] L. Gao, Y. Ding ,X. Zhai , H Min , G. Liu , R. Lan , Y. Shen "Passively Q-switched 2 μm laser based on graphene/BN heterostructure as saturable absorber." *Optics & Laser Technology* ,vol. 168p.p 109852, 2024.

[5] M. Erfani , M. Dehghan Baghi , M. Hajimahmodzadeh, M. Soltanolkotabi . "Pulsed Nd: YAG passive Q-switched laser using Cr^{+4}: YAG crystal." *Optics & Laser Technology* vol. 44 No.3, p.p 522-527, 2012.

[6] C. Li , Z. Gao , Z. Zhai , S. Ye and Y. Sun. "Growth and Passive Q-Switching Application of Cr: TiTe3O8 Crystal." *Crystals* , Vol. 12 No. 4 , p.p 558, 2022.

[7] J Tang, Z Bai, D Zhang, Y Qi, J Ding, Y Wang, Z Lu. "Advances in all-solid-level passively Q-switched lasers based on Cr^{+4}: YAG saturable absorber." In *Photonics* , (Vol. 8, No. 4, p. 93), 2021.

[8] X. Guo, S Tokita, K Fujioka, H Nishida, K Hirose, T Sugiyama, A Watanabe, K Ishizaki, "High-beam-quality, efficient operation of passively Q-switched Yb: YAG/Cr: YAG laser pumped by photonic-crystal surface-emitting laser", . *Applied Physics* ; vol. 123, p.p 1-6, 2017 .

[9] Y. Liu, W You, C Zhu, M Li, Y Sun, X Yin, D Chen, Y Feng, W Chen, X Yang, "A review of ns-pulsed Raman lasers based on diamond crystal"., *Frontiers in Physics*. Vol. *10*, No. 1054234 , 2022 .

[10] D. Tereshchenko, S. Smetanin, A. Papashvili, Y. Kochukov, A.Titov, E. Shashkov. "ASelf-Separation of a Single Ultrashort Light Pulse in the Parametric Raman Anti-Stokes Laser Based on a CaMoO4 Crystal under Intracavity Synchronous Pumping" . *Crystals*, vol.13, No.(4) p.p 636, 2023.

[11] X. Wang, X. Wang, J. Dong, "Sub-nanosecond, high peak power Yb: YAG/Cr4+: YAG/YVO4 passively Q-switched Raman micro-laser operating at 1134 nm". *Journal of Luminescence*, vol. *234*, No. 117955. 2021. https://doi.org/10.1016/j.jlumin.2021.117955

[12] D. Errandonea, R. Lacomba-Perales, K.K Mishra," A. In-situ high-pressure Raman scattering studies in PbWO4 up to 48 GPa". *Journal of Alloys and Compounds*., vol. *667*, p.p36-43, 2016.

[13] M Frank, S. Smetanin, M. Jelínek, D Vyhlídal, M. Kosmyna, A. Shekhovstov, K. Gubina "Stimulated Raman Scattering in Pb (MoO4) 1− x (WO4) x with x= 0, 0.5, 0.8 and 1.0 with Combined Frequency Shifts on High-and Low-Frequency Raman Modes under Synchronous Picosecond Laser Pumping" . *Crystals*, vol. *12*, No. (2), p.p148, 2021 .

[14] R. Lan, F. Zhang, Z Wang, W. Xiong, H. Yuan, T. Feng ,"Efficient near-infrared, multiwavelengths PbWO4 Raman laser". *Optical Engineering*, vol. *56* No.(9), P.P 096112-096112, 2017 . doi: 10.1117/1.OE.56.9.096112.

[15] D. Saad, A.M Salih " Rate Equations Model to Simulate the Performance of Passive Q-Switched Laser with Raman Medium Optical System". *Indian Journal of Science and Technology*, Volume: 16, Issue: 39, Pages: 3353-3360, 2023 .DOI: 10.17485/IJST/v16i39.1744

[16] Z. Hussein, A K M Salih.Investigation of Initial Transmission Effect on Saturable Absorber Optical Performance of Passive Q-Switching Doped Fiber Laser .*Neuro Quantology*. vol. 19No. (7), P.P 103-110, 2021 .

[17] T . Hussein, A. Salih , "Investigation of Effective Beam Area Ratio Effect on Characteristics of Passive Q-Switched Fiber Doped Laser" ,*Journal of Optoelectronics Laser*, Volume 41 Issue 10, 2022. DOI: 10050086.2022.10.47.

[18] V. Pérez-Alonso, R Weigand , "Powerful algebraic model to design Q-switched lasers using saturable absorbers". *Optics and Laser Technology*, vol. 164, p.p109506, 2023.

[19] Z.Hussein, AKM Salih, "Saturable absorber initial transmission effect on characteristics of passive Q-switching Er^{+3}doped fiber laser" *AIP Conference Proceedings*, vol. 2386 No. 080010, 2022.

[20] W. Chen , Y. Inagawa , T. Omatsu , M Tateda, N. Takeuchi , Y. Usuki , "diode-pumped self- stimulated, passively Q-switching Nd^{+3}:$pbwo_4$ Raman laser , *Optics & Laser Technology*," p.p , 401-407, 2001.

[21] M Chen, S Dai, H Yin, S Zhu, Z Li, Z Chen, "Passively Q-switched yellow laser at 589 nm by intracavity frequency-doubled c-cut composite Nd: YVO4 self-Raman laser" *Optics & Laser Technology* .vol. 133, 2021.

[22] R Lan,F Zhang, Z Wang, W Xiong, H Yuan, T Feng "Efficient near-infrared, multiwavelengths $PbWO_4$ Raman laser," *Optical Engineering*, Vol. 56, Issue 9,p.p. 096112, 2017.

[23] H. Hiba, A. A. Salmanb, M. A. Munshida , A. Al-Janabib. "Passive Q-switching using Lead Sulfide suspension as a saturable absorber in 1.5 μm region." *Optical Fiber Technology* vol. 52 ,p.p101969,2019